EARTH SCIENCES
RESEARCH JOURNAL

Earth Sci. Res. J. Vol. 24, No. 3 (September, 2020): 277-284

UNIVERSIDAD NACIONAL DE COLOMBIA

COMPUTER SCIENCE APPLIED TO GEOLOGY

Eruption Cycle of Volcanic Rocks Based on Virtual Reality Technology

Jiqiang Yang[1]*, Xing Wang[2]
[1]College of Creative Culture and Communication, Zhejiang Normal University, Jinhua 321000, China
[2]School of Physics and Physical Engineering, Qufu Normal University, Qufu 273165, China
*Corresponding author: yangjiqiang_zjnu@126.com

ABSTRACT

The eruption cycle of volcanic rocks based on virtual reality technology is studied to reveal the spatial distribution of volcanic rocks and the genetic relationship between different lithologic assemblages, and effectively guide volcanic exploration. Taking Xujiaweizi fault depression and Yingshan depression in Songliao Basin as the research area, the monocular vision method of virtual reality technology is used to collect data from the study area. Then, the three-dimensional dynamic scene of the study area was constructed. Based on this, combined with the research steps and division basis of the volcanic eruption cycle, the eruption cycle of the volcanic region in the study area is studied. According to the characteristics of volcanic activity, volcanic facies sequence, and rock rhythm combination in Xujiaweizi fault depression, the first and three sections of Yingcheng formation are divided into three eruption periods according to the contact relationship between sedimentary strata and volcanic rocks in the eruptive intermittent period. Y1C1, Y1C2, Y1C3, Y3C1, Y3C2, and Y3C3 are respectively from bottom to top. Yingshan volcanic rocks in Yingshan depression are divided into three cycles and six periods. Each stage has significant stages and differences, and the eruption intensity is different. The overall performance is gradually enhanced, and the internal cycle is characterized by the first strong and then weak.

Keywords: Virtual Reality; Monocular Vision; Volcanic Rock; Cycle; Eruption; Period.

Ciclo de erupción de rocas volcánicas con base en tecnología de realidad virtual

RESUMEN

Este estudio analiza el ciclo de erupción de las rocas volcánicas basado en tecnología de realidad virtual con el fin de revelar la distribución espacial de las rocas volcánicas y la relación genética entre diferentes conjuntos litológicos y, además, guiar efectivamente la exploración volcánica. Se definió la depresión de falla Xujiaweizi y la depresión de Yingshan en la cuenca Songliao como el área de investigación. El método de visión monocular de la tecnología de realidad virtual se utilizó para recopilar datos del área de estudio, y se construyó la escena dinámica tridimensional del área de estudio. Con base a esto, además de los pasos de investigación y la base de división del ciclo de erupción volcánica, se estudia el ciclo de erupción volcánica del área. De acuerdo con las características de la actividad volcánica, la secuencia de facies volcánicas y la combinación de ritmo de roca en la depresión de la falla Xujiaweizi, las tres secciones de la formación Yingcheng se dividen en tres períodos de erupción de acuerdo con la relación de contacto entre los estratos sedimentarios y las rocas volcánicas en el período eruptivo intermitente. Y1C1, Y1C2, Y1C3, Y3C1, Y3C2 y Y3C3 están, respectivamente, de abajo hacia arriba. Las rocas volcánicas de Yingshan, en la depresión de Yingshan, se dividen en tres ciclos y seis períodos. Cada etapa tiene diferencias significativas y la intensidad de la erupción es diferente. El rendimiento general se mejora gradualmente y el ciclo interno se caracteriza por primero fuerte y luego débil.

Palabras clave: Realidad virtual; Visión monocular; Roca volcánica; Ciclo; Erupción; Período.

Record
Manuscript received: 01/06/2019
Accepted for publication: 11/03/2020

How to cite item
Yang, J., & Wang, X. (2020). Eruption Cycle of Volcanic Rocks Based on Virtual Reality Technology. *Earth Sciences Research Journal*, 24(3), 277-284. DOI: https://doi.org/10.15446/esrj.v24n3.89468

ISSN 1794-6190 e-ISSN 2339-3459

https://doi.org/10.15446/esrj.v24n3.89468

Introduction

With the development of oil and gas exploration, volcanic oil and gas reservoirs have become an essential part of oil and gas exploration. Volcanic rocks are complex in rock type, uneven in regional distribution, and fast in lateral lithology. Volcanic oil and gas reservoir exploration technology is a difficult point in petroleum technology research today (Zhu et al., 2017). The volcanic gas reservoirs in the Songliao basin are controlled by space-time matching relationship between source rocks, volcanic traps, and fault transport channels, which provides a basis for finding desirable exploration areas for volcanic rocks. Stages and differences characterize the volcanic eruption, lithology, and structure are complex and diverse, and physical properties are different. Each facies belt has different lithological combinations, forming processes, diagenetic modes and structural structures, and has different pore structure characteristics. Volcanic eruption cycle study can reveal the spatial distribution of volcanic rocks and the genetic relationship among diverse lithologic assemblages, which provides useful guidance for volcanic exploration (Tian et al., 2017).

Chen Jianwen et al. found that oil and gas accumulation is not only related to the lithology of volcanic rocks, but also related to the general characteristics of volcanic rocks, and natural gas is usually enriched in the central part of volcanic structures. By Planke and others, the favorable reservoir is mainly distributed in the favorable lithofacies area of the volcanic crater near fire pass facies belt. In recent years, favorable lithologic and lithofacies zone drilling productivity has been found to be closely related to volcanic type. Tang Jianren et al. have discovered that volcanic reservoirs are controlled by volcanic structures and lithofacies. Different types of volcanic structures have different lithofacies distribution characteristics and hydrocarbon bearing properties. Therefore, studying the eruption cycle of volcanic eruption and defining the distribution characteristics and evolution rules of volcanic apparatus have important guiding and practical significance for volcanic oil and gas exploration.

Volcanic rocks are formed by magma rising from the weakest zone of the strata along the cut through basin basement and the deep fault of the crust. Compared with sedimentary rocks, volcanic rock deposits are not controlled by the accommodation of water bodies. The formation characteristics of this "water and fire" symbiosis make volcanic magma form superposed volcanic bodies in multi-stage and intermittent eruptions (Skelin et al., 2018). The change of volcanic rocks in material composition and lithology is the basis for dividing cycles and periods. In different volcanic eruption cycles or different periods of the same cycle, the material composition is different, resulting in the regularity of volcanic lithology in longitudinal direction, and the corresponding logging curve has the characteristics of prosodic variation (Yang et al., 2018). The seismic reflection characteristics of different lithological characteristics are different in continuity, stratification and amplitude intensity.

Songliao basin is a deep structural depression with large scale and controlled by tensional and torsional faults. Yingshan depression and Xujiaweizi fault depression are the main areas of deep natural gas exploration. The volcanic reservoirs are of strong heterogeneity and lateral variation. The separate volcanic reservoirs can form an independent reservoir forming system, which may appear in a plane with overlapping distribution. Favorable reservoirs are controlled by facies belts (Wendt et al., 2017), the exploration of volcanic gas reservoirs is rather difficult. In order to identify the macroscopic rules of the distribution of volcanic reservoirs in different stages of the study area, in order to guide the exploration of volcanic rocks, this paper divides the eruption characteristics of volcanic rocks in Songliao basin into cycles (Geurden et al., 2017). Due to the less drilling and core data in the study area, the virtual reality technology was used to collect the three-dimensional scene data of Songliao Basin, and the characteristics of the distribution and evolution of each sub volcano were obtained. Based on the study of the step and division of volcanic cycles, the eruption cycle of Songliao Basin was studied in detail, and the subsequent reservoir prediction and meticulous research were carried out. It has important guiding significance for the following reservoir prediction and fine research work.

Material and method

Survey of research areas

The study area is located in Songliao Basin. The deep layer of Songliao Basin consists of three first-order tectonic units: eastern fault depression zone, central paleo-uplift zone and western fault depression zone. Take the Xujiaweizi fault depression located in the northern Songliao Basin Eastern fault depression and the main part of Yingshan depression zone in the north of the Songliao Basin as the key research area, the volcanic eruption cycle study is carried out (Chen, 2017).

Xujiaweizi fault depression is close to the central paleo-uplift belt and is a deep and large-scale fault depression. It extends nearly north-south with a length of 90 km. The widest part in the middle is 5 km and its area is 4300 km^2. The fault depression is a single fault graben fault depression in the west to the east. It can be divided into many structural units, such as the western fault depression belt, the sag depression structural belt, the eastern slope zone, the funyue low uplift and the low uplift. According to the results of the third resource evaluation, the total deep resources of Xujiaweizi fault depression are 6772×108 m^3. As of the end of 2007, 10^5 wells were drilled in the deep part of the Xujiaweizi fault depression. A total of 5058.8 km^2 of pre-stack time migration processing has been completed in the deep layer, with a total proved natural gas reserve of 2457×108 m^3 handed in, with a proven rate of 36.2% (Bracquart et al., 2017).

Yingshan depression covers an area of 400 km^2, and its syncline and Xujiaweizi fault depression are divided by Chaoyang Valley anticline belt, which is an asymmetric graben type double fault depression under the control of four station fault and Linjiang fault. Before the deposition of the Doutlouku formation, the structure is controlled by volcanic action, forming two ancient landforms with four concave uplifts, namely, the Paleo uplift, the Qingshan uplift and the Yingshan depression. The north is a low-lying area. Before the deposition of the group, the North South differential subsidence further strengthened the southern structure, and the amplitude of the western Paleo long structure decreased. Up to now, strong tectonic inversion has occurred in the north, slight inversion in the south, and stable subsidence in the middle, resulting in the formation of today's surrounding high, middle low tectonic form. Yingcheng formation is located in the fault depression period of the basin. At present, there are five exploration wells in Yingshan depression. There are few logging and drilling data, and the overall exploration and development degree is weak (Pavey et al., 2017).

Research method for eruption cycle of volcanic rocks

Virtual reality technology is used to reconstruct the volcanic terrain in the study area, and the monocular vision method is applied to collect the data collected in the study area. The image machine is used as the image receiving collector to carry out the data measurement and acquisition in the research area needed for comprehensive three-dimensional modeling, such as image processing, data acquisition and visual capture. According to the three dimensional reconstruction data of dynamic scenes in the study area, combined with the research steps of volcanic eruption cycle and volcanic eruption cycle stages, the lithology, transport characteristics and lithofacies periodic changes of volcanic rocks in the study area were analyzed, and the results of the eruption cycle of volcanic rocks in the study area were obtained.

Three-dimensional reconstruction of dynamic scene in research area based on virtual reality technology

By using monocular vision method, the collected image can be either a single image of a single viewpoint or multiple images of several different viewpoints (Lozano-Bilbao et al., 2017). This method can recognize the degree of light and shade, texture lines, distance points, outlines and so on. This method is simple in equipment, simple in structure, and can reconstruct the three-dimensional model of the object using only a single or a few images. These matching points are used to describe and obtain the coordinate information points of the three-dimensional object in space, so as to realize the three-dimensional reconstruction of the research area (Sun, 2017).

(1) Design of photometric stereo vision virtual reality

Although conventional brightness methods can reconstruct a three-dimensional model from a single image, there is less data information available from a single image. Therefore, the SFS method was improved in Woodham, and the photometric stereo vision method (Englberger & Dörnbrack, 2018) was introduced. The method is based on the brightness equation, as shown in formula (1):

$$D_1-\alpha\left(O_i\sum_{j\in N(i)}\frac{g_i+g_j}{2}\left(d_j-d_i\right)+\left(1-O_i\right)\sum_{j\in N(i)}\frac{\psi_i^{'}+\psi_j^{'}}{2}\left(d_j-d_i\right)\right)=0 \quad (1)$$

In the formula: $\left(1-O_i\right)$ denotes the intensity coefficient of the light source reflected from the surface of the object; g_j is the normal vector of the kinetic energy of the object; g_i is the refraction vector of the light source, ψ_i is the image pixel; $\left(d_j-d_i\right)$ denotes the two-dimensional parametric transformation value, which is the value of the response acquisition data to ensure the integrity of the data in the process of data analysis; $j\in N(i)$ denotes the value range of the data acquisition point. Photometric stereo vision uses multiple sources of light to obtain multiple images of the same object. By combining the conjugate equations of different images, the normal vector g_j of the kinetic energy of the object and the refraction vector g_i of the light source can be solved. Finally, the three-dimensional shape of the object can be restored. So, the current methods basically use multiple (4-6) light sources for 3D reconstruction, using matrix representation as shown in formula 2.

$$GH=\begin{bmatrix}\sigma_1^2 & & & & & & 0\\ & \sigma_1^2 & & & & & \\ & & \sigma_2^2 & & & & \\ & & & \cdots & & & \\ & & & & \sigma_\alpha^2 & & \\ & & & & & \sigma_\alpha^2 & \\ 0 & & & & & & \sigma_\alpha^2\end{bmatrix} \quad (2)$$

In the formula, *GH* matrix represents the mode of data storage calculation and σ_1^- represents the number of convertible and simplified conditions of light source. Pixels simplified by transformation can ensure the clarity of the picture in the process of data conversion, and it is more suitable for multi-object acquisition data conversion under different conditions (Xiang et al., 2018).

The transformed data need to be distinguished before they can be used, as shown in formula (3):

$$\begin{bmatrix}X_1=\frac{\sqrt{2}}{4}X_0\begin{bmatrix}-\exp\left(-i\beta\right)+\exp\left(-i\beta\right)\\0\end{bmatrix}\\ X_2=\frac{\sqrt{2}}{4}X_0\begin{bmatrix}0\\-\exp\left(-i\beta\right)+\exp\left(-i\beta\right)\end{bmatrix}\\ X_3=\frac{\sqrt{2}}{4}X_0\begin{bmatrix}0\\-\exp\left(-i\beta\right)+\exp\left(-i\beta\right)\end{bmatrix}\\ X_4=\frac{\sqrt{2}}{4}X_0\begin{bmatrix}-\exp\left(-i\beta\right)+\exp\left(-i\beta\right)\\0\end{bmatrix}\end{bmatrix} \quad (3)$$

In the formula, $\exp\left(-i\beta\right)$ represents the high-order attribute distortion vectors after data transformation, which can reflect the validity of the transformation process; X_0 represents the variable parameters that data can effectively retain in the transformation process; X_1, X_2, X_3 and X_4 represent the conversion success rates.

Through the above process, the design data of photometric stereo vision virtual reality is obtained, and the image of information particle operator distribution is shown in Figure 1.

(2) Three-dimensional reconstruction

The principle of 3D reconstruction is mainly to get images from the RGB camera and the far-infrared camera in the same direction, so that the direction of the two cameras can be as parallel as possible. This will help reduce the amount of computation when the camera is corrected, and get the RGB and depth images (Zhang et al., 2019) respectively. In order to solve the problem of image center deviation caused by different positions of two cameras, RGB images are first transformed into coordinates to align with the depth image coordinates. Then the coordinate positions of space points *x* and *y* are calculated. Finally, the three-dimensional coordinate point cloud data (*x*, *y*, *z*, *R*, *G*, *B*)is displayed through LOD hierarchical model, as shown in formula (4):

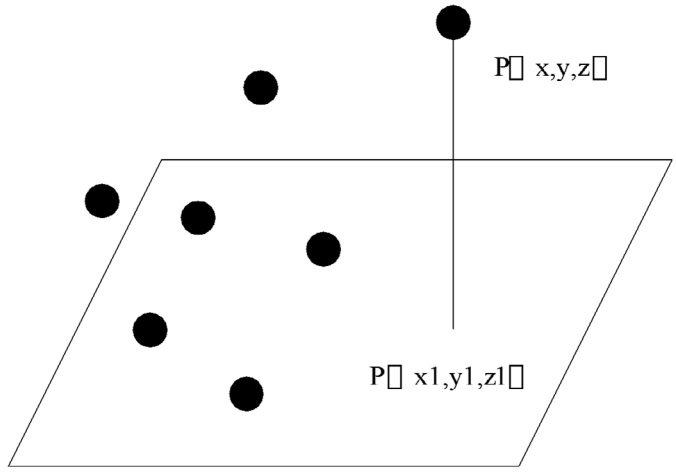

Figure 1. Information particle operator distribution

$$\begin{aligned}\left(x-x_1\right)+\Delta x&=-f\left(\frac{a_1\left(x-x_1\right)+b_1\left(y-y_1\right)+c_1\left(z-z_1\right)}{a_3\left(x-x_2\right)+b_2\left(y-y_2\right)+c_3\left(z-z_2\right)}\right)\\ \left(y-y_0\right)+\Delta x&=-f\left(\frac{a_2\left(x-x_1\right)+b_2\left(y-y_1\right)+c_2\left(z-z_1\right)}{a_3\left(x-x_2\right)+b_2\left(y-y_2\right)+c_3\left(z-z_2\right)}\right)\end{aligned} \quad (4)$$

In the formula: $\left(x-x_1\right)$ is the differential prime of one-dimensional coordinates of the model; $\left(y-y_0\right)$ is the data validation level variable of two-dimensional coordinates of the model. After the first display, the collected data will be allocated to a certain area. After the display, the collected data can be calibrated by photometric stereo YYUE. The process is shown in formula (5):

$$\begin{cases}x=S+a_0+a_1S+a_2L\\ y=L+b_0+b_1S+b_2L\end{cases} \quad (5)$$

In the formula, a_0, a_1 and a_2 are the three-dimensional coordinate valid values of points in the photometric stereo YYUE calibration process, and *S* is the optimum photometric stereo YYUE calibration parameter value. The point coordinates *ML*(*x*, *y*) and *F*(*x*, *y*) can be obtained intuitively, which greatly improves the occurrence of visual disturbance and ensures the three-dimensional dynamic rendering of the dynamic scene in the study area (Rocholl et al., 2017). The effect of three-dimensional reconstruction of the scene in the study area is shown in Figure 2.

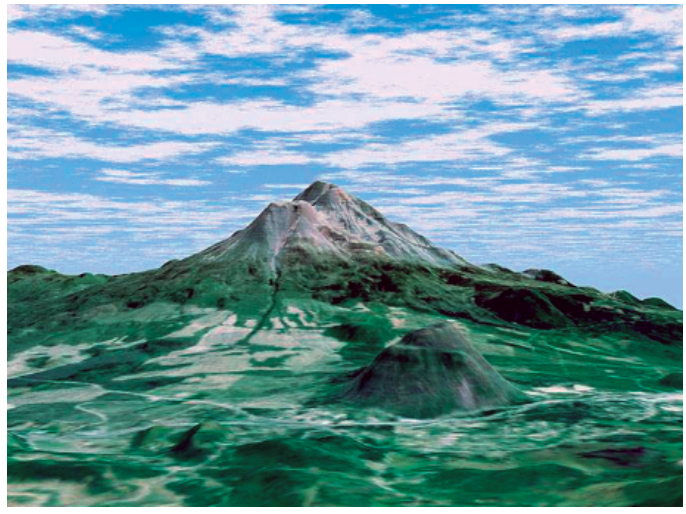

Figure 2. Scene 3-D reconstruction effect map of research area

Study on volcanic cycles

Study on the step of volcanic cycle

According to the 3D reconstruction data obtained from virtual reality technology in the study area, the same volcanic cycle in the volcanic strata in the study area is represented by a set of transitional lithological assemblages, and there are obvious changes in the occurrence of different volcanic cycles. Therefore, the interface of the cycle is manifested as an integrated surface from an unconformity to a sedimentary area in the volcanic area. On the top of the interface, volcanic rocks are obviously overlying. The thickness of a volcanic cycle is generally more than 80m, which can be used for lateral correlation of volcanic cycles with seismic profiles. In the cycle, we can use single well phase contrast (Zhou et al., 2017) according to the change of lithofacies. The steps of the study of volcanic cycles and phases are: (1) comprehensively using coring and thin slices to identify various data, determine the rock types and the lithofacies types of coring segments in the area, and identify all kinds of geological interfaces (weathering crust, volcanic ash layer and sedimentary interlayer); (2) Make full use of oil field drilling, logging and logging data to establish single well volcanic lithologic columnar section, according to rock assemblage. (3) Based on the classical volcanic activity facies sequence model, the primary division of volcanic cycles and stages of single well is carried out flexibly; (4) Based on the results of the zircon dating and the division and correlation of volcanic cycles and periods, we should set up separate wells and intervals and push them out according to the principle of "proximity" in order to clarify the eruption cycle and eruption period of the whole area.

Classification basis

The division of volcanic eruption periods should be based on the principle of isochronous comparison and hierarchical control, that is, in the same eruption cycle, the lithology, lithofacies, electricity, eruption sedimentary cycle and seismic reflection characteristics can be divided into two parts (Bolgar et al., 2018). The recognition of volcanic eruption stage should pay attention to unconformity, weathering crust, volcanic rock composition, color, structure, sedimentary rock interlayer, and so on, and combine seismology, geology and logging. In addition, the periodic changes of volcanic facies and the cyclical changes of volcanic components, such as volcanic channel facies, explosive phases, intrusive facies, overflow facies, volcanic sedimentary facies, periodic variations of basic, neutral and acidic volcanic rocks, and alkaline and subalkaline periodic changes are also the basis for dividing volcanic eruption stages (Liu et al., 2017).

Results

The eruption period of volcanic rocks in the Xujiaweizi fault depression.

Lithology and prosody characteristics of volcanic rocks

In different stages of volcanic activity, volcanic matter composition, different eruption modes, energy differences, and later crystallization and differentiation make each stage of volcanic rock have different lithological types, showing a certain prosody feature in lithological combination and logging response characteristics. The periodic variation of volcanic lithology and the characteristics of rhythmic combination are the reflection of the intensity of volcanic eruption, so it can be used to divide volcanic eruption times. Photographs of volcanic cores at different eruption stages are shown in Figure 3. The lithology and logging response characteristics of different types of volcanic rocks are shown in Figure 4.

The same period of secondary volcanic rocks in Xujiaweizi fault depression usually has the following lithologic variations:

(1) Mainly volcaniclastic. Usually the central eruption or central fissure eruption, its eruption energy is strong, the eruption product is mainly volcaniclastic, and has positive rhythmic lithological characteristics. In general, volcanic eruption material is composed of caking, volcanic breccia and tuff at the top. Figure 3 (a) is the third stage volcanic rock of the Sheng Shen 2 well with this lithological feature. The electrical characteristics of this kind of combination, such as Xushen 8 well, are shown in Figure 4 (a). From the

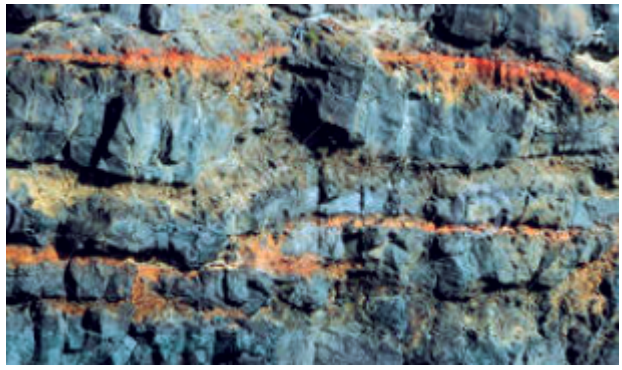

(a) Sheng Shen Geng 2 Well, 2902.67 m

(b) Sheng Shen Geng 203 Well, 3006.5 m

Figure 3. Core photographs of volcanic rocks at different eruption stages

electrical characteristics of Xushen 8 well, the block rock has high resistivity, medium and low natural gamma, while the top tuff has low resistivity and high natural gamma. The top and bottom of this type of volcanic lithologic assemblage are usually volcanic sedimentary rocks or tuff, and the electrical characteristics are the decrease of resistivity and the increase of natural gamma, indicating the beginning and end of a volcanic eruption.

(2) Lava is dominant. The energy of fissure eruptive volcanic rocks is weak, and the eruptive products are mainly volcanic lavas, which generally contain only a small amount of pyroclastic rocks. This lithologic assemblage usually occurs in the Shengping-Anda area and the southern Fung Lok area in the northern part of the Xujiaweizi fault depression. The volcanic lavas are mainly dominated by acid rhyolite, while the northern part of the andesite is dominated by basic basalt and neutral andesite (Zong et al., 2018). Figure 3 (b) core image of the Shenshengeng 203 well shows that the top of the lava is usually very porous, reflecting the end of the eruption of the volcanic eruption, and the lava exposing the surface; at the end of the eruption, due to weathering and surface water communication, the pores on the top of lava are very developed. These large numbers of primary stomata are signs of the end of the eruption period.

Figure 4 (b) shows the lithology and electrical characteristics of the basic lava in the northern part of the study area. It can be seen that the third stage volcanic rocks in Dashen 6 well are mainly basalts with a small amount of andesite. It has the characteristics of high resistivity and low natural gamma. Figure 4 (c) shows the lithological and electrical characteristics of acid lava in the central and southern part of the study area. It can be seen that the second stage of Shengshen 4 well is mainly fissure eruption, and the rock type is mainly rhyolite. If the lithologic assemblage of these volcanic rocks is thicker, the middle part tends to show higher natural gamma and high resistivity characteristics. The top and bottom are usually volcanic sedimentary rocks or tuff, and the electrical characteristics are the decrease of resistivity and the increase of natural gamma, indicating the beginning and end of the eruption.

(3) The interbedding of lava and pyroclastic. The energy of volcanic eruption in the center fissure type is slightly weaker than that in the center. Volcanic eruption products are usually dominated by pyroclastic and lava, indicating that the energy of volcanic eruption from strong to weak or weak to strong. As shown in Figure 4 (d), the deep well of WangShen 903, with low energy at the beginning of the eruption, is dominated by rhyolite, and then gradually increases, the volcanic ejecta is breccia, and then the energy gradually weakens. Overall, the process of weakening one strong and one weak indicates the ending of a volcanic activity.

Variation based on the volcanic lithofacies belt cycle

In the same period, the cyclical changes of volcanic rock composition, structure and structure make volcanic rocks exhibit certain prosody features. These prosody features overlap or appear repeatedly, reflecting the pattern and output pattern of spatial distribution of volcanic eruption in the same period, and the appearance characteristics of these products, which is the "facies" of volcanic rocks (Cheng et al., 2017). Each stage of volcanic rock is usually composed of one or more phase sequences, showing a continuous or quasi continuous phase sequence.

A complete volcanic facies sequence assemblage in the longitudinal direction is volcanic channel facies - explosive phase overflow facies - intrusion facies - volcanic sedimentary facies. In fact, only 2-3 lithofacies types or single lithofacies types can be found in the facies sequence assemblages, and the phenomenon of duplication or inversion may also occur. The change of phase sequence is actually the manifestation and result of the process of volcanic activity. Therefore, the periodic variation of phase sequence can be used as a basis for dividing volcanic eruption periods.

Volcanic facies in Xujiaweizi fault depression are usually divided into 5 subfacies, 15 facies subfacies, including volcanic channel facies, outburst facies, overflow facies, intrusive facies and volcanic deposits. Each facies zone is subdivided into 3 sub facies. If the eruption energy of the volcano is strong in the early stage and weakened in the later stage, and the eruption time is long, there may be a complete phase sequence combination near the crater. If the energy of the volcanic eruption is weak in the initial stage and strong in the late stage, the combination of the phase sequence will be reversed (Peng et al., 2016). The phase sequence changes of volcanic rocks in Yingcheng formation of Xujiaweizi fault depression mainly begin with explosive facies or overflow facies, and seldom start by volcanic channel facies. Moreover, the volcanic sequence assemblages are usually composed of 2-3 facies belts, and the complete facies assemblages are rare. The characteristics of different eruptive subvolcanic facies in Xujiaweizi fault depression are shown in Table 1.

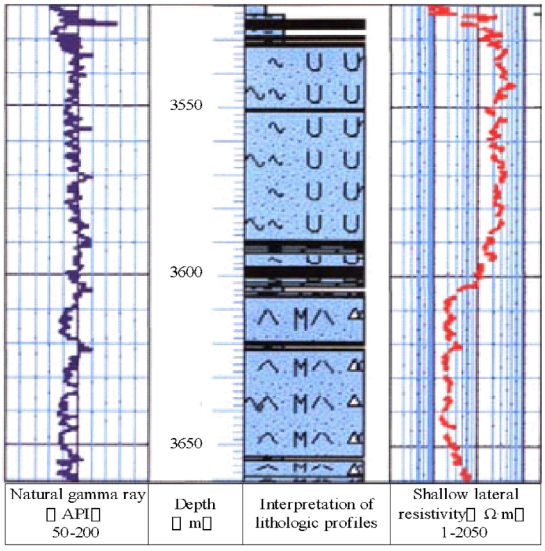

(a) Xushen 8 well

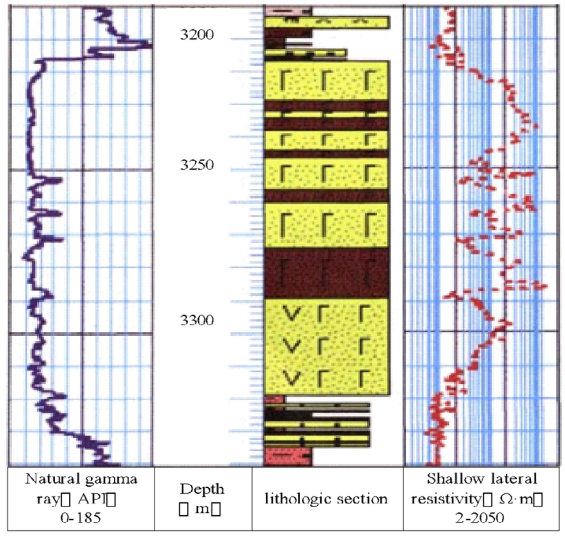

(b) Dashen 6 well

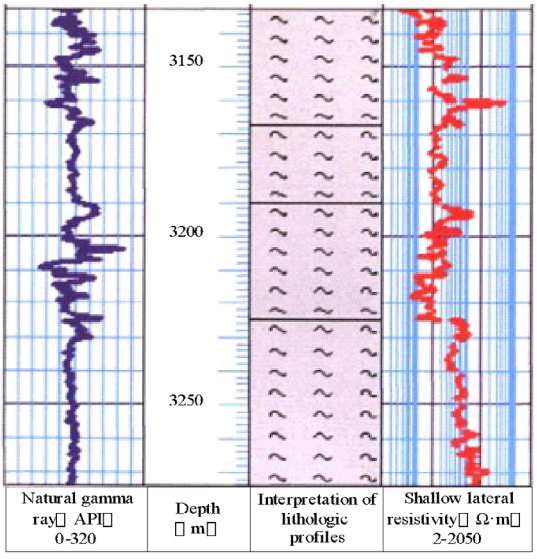

(c) Shengshen 4 well

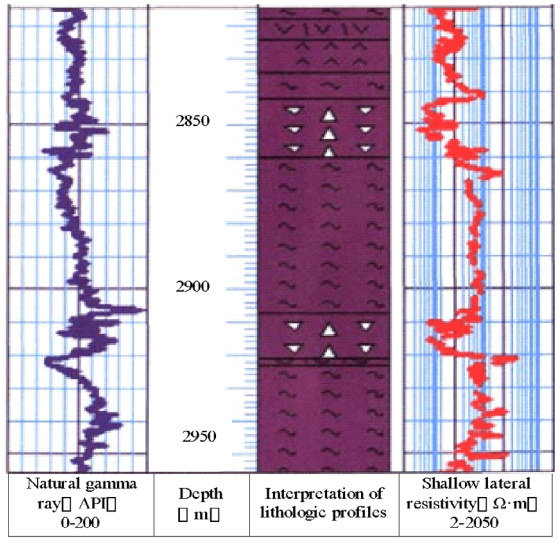

(d) Wangshen 903 well

Figure 4. Lithology and logging response characteristics of different types of volcanic rocks

Table 1. Lithofacies association and variation characteristics of subvolcanic rocks at different eruption stages in Xujiaweizi fault depression

Representative well	Well DA Shen 1			Well Wang Shen 1			Well Xu Shen 8			Xu Shen 9 well		
Eruption period	Phase I of Yingsan Section	Phase II of Yingsan Section	Phase III of Yingsan Section	Phase I of Yingsan Section	Phase II of Yingsan Section	Phase III of Yingsan Section	Phase I of Ying Phase I	Phase II of Ying Phase I	Phase III of Ying Phase I	Phase I of Ying Phase I	Phase II of Ying Phase I	Phase III of Ying Phase I
Volcanic activity intensity	Strong-weak	Strong-strong	Weak-strong- weak	Weak-strong- weak	Strong-weak	Strong-weak	Strong-intermittence	Strong-weak	Strong-intermittence	Strong-weak	Strong-weak	Weak-strong-intermittent
Types of Phase Sequence Combination	Explosive-overflow facies	Spillway-explosive facies	Overflow-explosive phase superposition	Overflow-explosive phase superposition	Explosive-overflow facies	Explosive-overflow facies	Explosive-overflow facies	Explosive-overflow facies	Volcanic channel facies-explosive facies	Explosive-overflow facies	Eruptive facies-volcanic sedimentary facies	Eruptive-overflow-volcanic sedimentary facies
Eruption mode	Fissure type			Fissure type			Central type			Fissure type		

Division result

From the analysis of lithologic combination and electrical characteristics of these volcanic rocks, we can see that at the beginning and end of the first eruption, the lithology changes are volcanic sedimentary rocks (or tuff) - pyroclastic rocks (or lavas) - volcanic sedimentary rocks (or tuff). The characteristics of electricity are the decrease of density and resistivity, and the increase of natural gamma (Wang et al., 2020). These characteristics are the signs of volcanic intermission. On the basis of lithology and facies combination, according to the regularity of volcanic activity and the particularity of volcanic strata, and combining the characteristics of volcanic lithology, lithologic assemblage, volcanic facies belt, sedimentary rock intercalation and electrical characteristics of the core and volcanic eruption, the first and three sections of Yingcheng formation in Xujiaweizi fault depression are divided into 3 eruption periods, followed by Y1C1, Y1C2 and Y. 1C3, Y3C1, Y3C2, Y3C3. The results are shown in Table 2.

Eruption stages and characteristics of volcanic rocks in Yingshan depression

The volcanic eruption cycle of Yingshan depression in the study area experienced a quiet period of intense volcanic eruption and quiet period of volcanic activity, while sedimentary intercalation is the representative lithology of the quiescence period and the most obvious indicator of the interface of the cycle. The eruption characteristics of volcanic rocks in Yingshan depression are shown in Table 3.

Cycle 1 is divided into stages 1 and 2 from bottom to top. The period 1 is mainly neutral or moderately acidic volcanic rocks. It shows layered like reflection in seismic sections. Sedimentary facies and sedimentary tuff are the main sedimentary facies in stage 2, and the thickness of sedimentary interbeds is about 150m. It can be used as volcanic eruption times alone, indicating volcanic eruption into a long quiet period. The activity of Fire Mountain is from strong to weak, and it shows good stratification and continuity in seismic profile, and is easy to track and compare horizontally.

At the top of the cycle 2, there is a thin sedimentary rock with a thickness of about 50m, showing a continuous strong reflection coaxial axis on the seismic profile, which is the interface between cycle II and cycle III, indicating that the two cycles experienced only a relatively short eruption period. On the whole, the cycle 2 is mainly volcanic rock, and from bottom to top, it is divided into stage 3 and stage 4. Three of them were mainly volcanic lava or volcanic breccia, locally developed fluffy tuff and granularity. Phase 4 was mainly composed of fused tuff and rhyolite tuff, with smaller granularity. It showed that the eruption of multi crater gradually evolved into the eruption of large scale volcanic eruptions. The obvious alteration of granularity and lithology of these volcanic rocks indicates the vertical migration eruption of volcanic rocks at GR. The curves show rhythmic changes, and the reflection of the upper part relative to the lower part of the layer is disorderly on the seismic section.

Cycle 3 is divided into stages 5 and 6 from bottom to top. The stage5 is dominated by rhyolite and rhyolite breccia lava, and the granularity is large. Stage 6 is mainly tuff, with smaller granularity, indicating vertical migration and eruption of volcanic rocks. Volcanic activity gradually ends, and the upper part of the seismic section shows relatively good stratification, while the lower

Table 2. Volcanic eruption stages in Xujiaweizi fault depression, Songliao Basin

Stratum	Ying one section			Ying two section	Ying three section		
Lithology	Rhyolitic debris tuff, rhyolitic breccia, tuff agglomeration, fused breccia			Tuffaceous sandstone, mudstone, conglomerate and silty conglomerate	Andesite, andesite basalt, diorite porphyrite and tuffaceous mudstone		
Phase sequence combination	Spillover facies dominates	Eruptive phase	Eruptive phase	Lacustrine fan delta facies	Overflow phase	Volcanic sedimentary facies Overflow phase	Overflow phase
Eruption period	Y_1C_1	Y_1C_2	Y_1C_3	Volcanic-sedimentary cycle	Y_3C_1	Y_3C_2	Y_3C_3
Cycle	Eruption cycles I			Depositional cycle	Eruption cycles II		
Representative well	Xu Shen 1 well	Well Xu Shen 6		Xudong area	Well Da 2 well		

Table 3. Characteristics of each eruption period of volcanic rocks in Yingshan Depression

Cycle		Cycle I		Cycle II		Cycle III	
Period		Period 1	Period 2	Period 3	Period 4	Period 5	Period 6
Lithologic characteristics		Neutral or intermediate-acid volcanic rocks predominate	Sedimentary rock or tuff	Fused tuff is locally developed mainly from volcanic lava or volcanic breccia with large grain size.	Fused tuff and rhyolitic tuff are the main types.	Rhyolite and rhyolitic breccia are dominant with larger grain size.	Tuff is the main type
Earthquake Reflection characteristics		Layer-like reflection with thinner formation thickness	Good stratification, continuous and clear reflection in-phase axis	Intermittent and disorderly reflection, poor stratification, large bottom thickness	Intermittent reflection is better than continuous reflection and stratification is better.	The reflection is chaotic and worm-like, with poor stratification and large formation thickness.	The formation thickness is thin and the stratification is relatively good.
Stratigraphic Contact Relation		The stratum overlaps the Sizhan fault and partially exceeds T41.	The stratum overlaps the Sizhan fault and partially exceeds T41.	The stratum overlaps the Sizhan fault and partially exceeds T41.	The stratum overlaps the Sizhan fault and partially exceeds T41.	Load cutting, local strata overlap the Fourth Station Fault	The stratum overlaps the Sizhan fault
Interface marker	Cyclic interface	Intermittent depositional interlayer with larger thickness			Intermittent depositional interlayer with smaller thickness		
	Periodic interface	1. Volcanic metamorphic sedimentary rocks 2. Better stratification and continuity of seismic reflection characteristics		1. The size of volcanic rocks decreases 2. Better seismic reflection characteristics		1. The size of volcanic rocks decreases 2. Better seismic reflection characteristics	
Volcanic apparatus	Total area (km^2)/Number (individual)/ Maximum amplitude/(m)	25.36/8/71	31.78/10/37	149.19/25/91	82.14/20/100	151.71/15/121	73.31/18/161
	Distribution location	Sporadically distributed near Well-4	Sporadic distribution at the edge	Large area is distributed in the middle and south, along the fault	Small area in central and Northern China	Widespread distribution in the West	Small areas are distributed in the West and south

part reflects chaos and vermicular reflection, and the stratification is poor. On the whole, the first stage is controlled by the four station fault, the sub top interfaces are overlapped to the four station fault, and the area is above the first bottom interface.

Discussions

Volcanic eruption period is a relatively continuous volcanic activity. Its material composition and eruption intensity also have regular changes in the longitudinal direction. A volcanic eruption cycle consists of multiple eruption periods. The lithology and seismic profile characteristics of the same cycle differ from each other, such as volcanic lithology change, volcanic particle size change and seismic reflection characteristics change, etc., which is the basis of the internal division period of the cycle (Bergroth et al., 2018). In this paper, the virtual reality technology is used to study the eruption cycle of volcanic eruption in the Xujiaweizi fault depression and Yingshan depression. The data of the study area are collected by monocular vision based on the 3D reconstruction of the virtual reality technology, which ensures data blocking, avoids the transition of the connected data, and ensures the maximum degree of clarity. The dynamic state of data such as texture and transparency can achieve the best imaging state and realize the dynamic rendering of 3D scene in the study area. On this basis, the eruption cycle times of volcanic rocks in the study area are divided according to the classification steps and division basis of the cycle stages.

During the Mesozoic, the study area experienced the regional tectonic evolution of "North-South strike, east-west subduction, mantle crust, and opening and closing alternation", and 3 major volcanic eruptions occurred in succession, namely, Jurassic flint rock formation and Cretaceous Yingcheng formation. Each volcanic eruption cycle has erupted intermittently. Compared with the eruption cycle, the eruption period is much shorter than that of the first cycle. A volcanic eruption cycle is usually composed of multiple eruption periods (Zhou & Zhang, 2017). The same sub volcanic rocks in Xujiaweizi fault depression usually have three lithologic variation assemblages, mainly volcaniclastic, mainly lava and interbedding of lava and pyroclastic rocks. They reflect the rhythmic characteristics of lithological assemblage and logging response, reflecting the strong and weak eruption of volcanoes. In the same period, volcanic eruption materials are spatially distributed volcanic rocks. Finally, the first and three sections of Yingcheng formation in the Xujiaweizi fault depression are divided into 3 eruption periods, followed by Y1C1, Y1C2, Y1C3, Y3C1, Y3C2 and Y3C3. The Yingshan section of Yingshan depression

in the study area is divided into three cycles, i. e., cycle 1, II and III, which can be subdivided into six stages. Among them, cycle I develops large sets of sedimentary rock intercalations, showing obvious stratification, high continuity and stable equilibrium and strong amplitude energy characteristics in seismic profiles. Cycle II only develops a thin sedimentary interlayer on the top, showing only a continuous strong reflection axis on the seismic profile, but it is obviously different from the chaotic reflection characteristics of the volcanic rocks. The lateral correlation of volcanic eruption cycles can be achieved. The eruption of volcanic rocks has obvious stages and differences. The intensity of each eruption is different, and the overall performance is gradually enhanced.

Conclusions

Volcanic activity is characterized by polycyclic and multi-stage activities. The magmatic products of a volcanic activity cycle and their volcanic structural traces have certain unity and coordination in time and space distribution. Volcanic rocks of different stages of the same cycle, or volcanic rocks of different stages of the same period, are different in volcanic lithofacies zones due to different energy and eruption modes. Different volcanic lithofacies zones control the development of reservoirs and the enrichment and high production of oil and gas. Therefore, by using virtual reality technology to build three-dimensional dynamic scenes in the study area, it is of great significance to study volcanic eruptions cycles times and effectively divide volcanic eruption stages to identify favorable facies zones of volcanic rocks, analyze the inducing factors of reservoir development, and hydrocarbon distribution and accumulation rules.

References

Bergroth, J. D., Koskinen, H. M. K., & Laarni, J. O. (2018). Use of immersive 3-D virtual reality environments in control room validations. *Nuclear Technology*, 02, 1-12.

Bolgar, F., Eames, E., Hottier, C., & Semelin, B. (2018). Imprints of quasar duty cycle on the 21 cm signal from the Epoch of Reionization. *Monthly Notices of the Royal Astronomical Society*, 478, 5564-5578.

Bracquart, B., Mareau, C., Saintier, N., & Morel, F. (2017). Experimental study of the impact of geometrical defects on the high cycle fatigue behavior of polycrystalline aluminium with different grain sizes. *International Journal of Fatigue*, 109, 17-25.

Chen, C. J. (2017). Application of virtual local area network technology in smart grid. *Chinese Journal of Power Sources*, 41, 1646-1648.

Cheng, C., Liu, Z., Guo, Z., & Debnath, N. (2017). Waste-to-energy policy in China: A national strategy for management of domestic energy reserves. *Energy Sources Part B-Economics Planning and Policy*, 12(10), 925-929.

Englberger, A., & Dörnbrack, A. (2018). Impact of the diurnal cycle of the atmospheric boundary layer on wind-turbine wakes: A numerical modelling study. *Boundary-Layer Meteorology*, 166, 423-448.

Geurden, T., Bartram, D. J., Vanimisetti, H. B., Fanke, J., Camuset, P., Devos, J., Sawyer, A., Von Samson-Himmelstjerna, G., Demeler, J., & Charlier, J. (2017). A multi-country study to assess the effect of a treatment with moxidectin pour-on during the dry period on milk production in dairy cows. *Veterinary Parasitology*, 237, 104-109.

Liu, C. H., Qi, Y., & Ding, W. R. (2017). Infrared and visible image fusion method based on saliency detection in sparse domain. *Infrared Physics & Technology*, 83, 94-102.

Lozano-Bilbao, E., Gutierrez, A. J., Hardisson, A., Rubio, C., Gonzalez-Weller, D., Aguilar, N., Escanez, A., Espinosa, J. M., Canales, P., & Lozano, G. (2017). Influence of the submarine volcanic eruption off El Hierro (Canary Islands) on the mesopelagic cephalopod's metal content. *Marine Pollution Bulletin*, 129, 474-479.

Pavey, T. G., Kolbe-Alexander, T. L., Uijtdewilligen, L., & Brown, W. J. (2017). Which women are highly active over a 12-year period? A prospective analysis of data from the australian longitudinal study on women's health. *Sports Medicine*, 47, 1-14.

Peng, W., Liu, Z., Motahari-Nezhad, M., Banisaeed, M., Shahraki, S., & Beheshti, M. (2016). A detailed study of oxy-fuel combustion of biomass in a circulating fluidized bed (CFB) combustor: Evaluation of catalytic performance of metal nanoparticles (Al, Ni) for combustion efficiency improvement. *Energy*, 109, 1139-1147.

Rocholl, A., Schaltegger, U., Gilg, H. A., Wijbrans, J., & Böhme, M. (2017). The age of volcanic tuffs from the Upper Freshwater Molasse (North Alpine Foreland Basin) and their possible use for tephrostratigraphic correlations across Europe for the Middle Miocene. *International Journal of Earth Sciences*, 107, 1-21.

Skelin, M., Lucijanić, T., Liberati-Čizmek, A. M., Klobučar, S. M., Lucijanić, M., Jakupović, L., Bakula, M., Lončar, J. V., Marušić, S., Matić, T., Romić, Z., Dumić, J., Rahelić, D. (2018). Effect of timing of levothyroxine administration on the treatment of hypothyroidism: a three-period crossover randomized study. *Endocrine*, 62, 432-439.

Sun, B. G. (2017). Revenue optimization algorithm for IaaS providers based on alliance perception in hybrid cloud environment. *Journal of Jilin University (Science Edition),* 55, 1491-1498.

Tian, Y., Xiao, Z., Wang, H., Peng, X., Guan, L., Huangfu, Y., Shi, G., Chen, K., Bi, X., & Feng, Y. (2017). Influence of the sampling period and time resolution on the PM source apportionment: Study based on the high time-resolution data and long-term daily data. *Atmospheric Environment*, 165, 301-309.

Wang, G., Wang, F., Shen, F., Jiang, T., Chen, Z., & Hu, P. (2020). Experimental and optical performances of a solar CPV device using a linear Fresnel reflector concentrator. *Renewable Energy*, 146, 2351-2361.

Wendt, A., Tassara, A., Báez, J. C., Basualto, D., Lara, L. E., & Garcia, F. (2017). Possible structural control on the 2011 eruption of Puyehue-Cordón Caulle Volcanic Complex (southern Chile) determined by InSAR, GPS and seismicity. *Geophysical Journal International*, 208, 134-147.

Xiang, Y., Cai, J., Guan, Y., Liu, W., Han, Y., & Liang, Y. (2018). Study on the configuration of bottom cycle in natural gas combined cycle power plants integrated with oxy-fuel combustion. *Applied Energy*, 212, 465-477.

Yang, Z. W., Chen, G. D., Wang, N., & Lin, H. (2018). Realistic simulation of heart display in virtual surgery. *Computer Simulation*, 35, 334-339.

Zhang, D. P., Xu, P. L., & Ge, L. Q. (2019). Research on quality assessment of elevator maintenance based on virtual technology. *Automation & Instrumentation*, 231, 42-44.

Zhou, C., Xu, H. D., Liu, H., & Li, C. (2017). Research on islanding detection methods for grid-connected distributed generation. *Journal of Power Supply*, 15, 125-131.

Zhou, X. L., & Zhang, H. (2017). The study on the model of periodic BIT data analysis relation to time sequence. *Journal of China Academy of Electronics and Information Technology*, 12, 128-131.

Zhu, Z., Ma, Y., Qu, Z., Fang, L., Zhang, W., & Yan, N. (2017). Study on a new wet flue gas desulfurization method based on the Bunsen reaction of sulfur-iodine thermochemical cycle. *Fuel*, 195, 33-37.

Zong, H., Cao, Y., & Liu, Z. (2018). Energy security in Group of Seven (G7): A quantitative approach for renewable energy policy. *Energy Sources Part B-Economics Planning and Policy*, 13(3), 173-175.